

AD-A204 889

THE ANALYSIS OF SOME UNDERSEA NOISE WITH APPLICATIONS
TO DETECTION(U) PRINCETON UNIV NJ INFORMATION SCIENCES
AND SYSTEMS LAB P WILLETT ET AL OCT 86

171

UNCLASSIFIED

N00014-81-K-0146

F/G 17/1

NL



DTIC
FILMED
4-87

1·0

2·8

2·5

1·5

3·15

2·2

1·1

1·2

3·5

2·0

1·3

4·0

1·4

4·5

1·8

1·25

1·4

1·6

AD-A204 889

SECURITY CLASSIFICATION OF THIS PAGE (When Data Entered)

DTIC FILE COPY 4

REPORT DOCUMENTATION PAGE		READ INSTRUCTIONS BEFORE COMPLETING FORM
1. REPORT NUMBER	2. GOVT ACCESSION NO.	3. RECIPIENT'S CATALOG NUMBER
4. TITLE (and Subtitle) The Analysis of Some Undersea Noise with Applications to Detection		5. TYPE OF REPORT & PERIOD COVERED Preprint
7. AUTHOR(s) Peter Willett and John B. Thomas		6. PERFORMING ORG. REPORT NUMBER
9. PERFORMING ORGANIZATION NAME AND ADDRESS Information Sciences and Systems Laboratory Department of Electrical Engineering Princeton University, Princeton, NJ 08544		8. CONTRACT OR GRANT NUMBER(s) N00014-81-K-0146
11. CONTROLLING OFFICE NAME AND ADDRESS Office of Naval Research (Code 411SP) Department of the Navy Arlington, VA 22217		10. PROGRAM ELEMENT, PROJECT, TASK AREA & WORK UNIT NUMBERS NR SRO-103
14. MONITORING AGENCY NAME & ADDRESS (if different from Controlling Office)		12. REPORT DATE October 1986
		13. NUMBER OF PAGES 10
		15. SECURITY CLASS. (of this report) Unclassified
		15a. DECLASSIFICATION/DOWNGRADING SCHEDULE
16. DISTRIBUTION STATEMENT (of this Report) Approved for public release; distribution unlimited		
17. DISTRIBUTION STATEMENT (of the abstract entered in Block 20, if different from Report) S DTIC ELECTE FEB 28 1989 D		
18. SUPPLEMENTARY NOTES Appears in the Proceedings of the Twenty-fourth Annual Allerton Conference on Communications, Control, and Computing, Urbana, IL, Oct. 1-3, 1986; pp. 266-275.		
19. KEY WORDS (Continue on reverse side if necessary and identify by block number) from 20 → merchant noise, shrimp noise, Johnson noise, nonlinear detectors. ljh		
20. ABSTRACT (Continue on reverse side if necessary and identify by block number) → This paper treats a signal detection problem using real noise records. The authors have had access to two medium-sized (each about 100000 samples) data sets, each from a non-Gaussian marine environment. The first, collected near a merchant shipping lane, has lower-than-Gaussian probability of high-amplitude observations (light tails). This appears to be due to the presence of a powerful narrowband component; when this is removed by an adaptive notch filter, the tails become heavier. The second, collected near a shrimp bed, has extremely heavy tails and a kurtosis (normalized fourth moment) of 82. Excel-		

DD FORM 1 JAN 73 1473

EDITION OF 1 NOV 65 IS OBSOLETE
S/N 0102-LP-014-6601

(Cont.)

SECURITY CLASSIFICATION OF THIS PAGE (When Data Entered)

(Cont.)

→ lent results are achieved through use of a Johnson noise model fit.

Keywords: → to field 19

DTIC
ELECTE
199808

2

D

THE ANALYSIS OF SOME UNDERSEA NOISE WITH APPLICATIONS TO DETECTION

Peter Willeit
University of Connecticut
Storrs, CT 06268.

and
John Thomas
Princeton University
Princeton NJ 08544.

Abstract

This paper treats a signal detection problem using real noise records. The authors have had access to two medium-sized (each about 100000 samples) data sets, each from a non-Gaussian marine environment. The first, collected near a merchant shipping lane, has lower-than-Gaussian probability of high-amplitude observations (light tails). This appears to be due to the presence of a powerful narrowband component; when this is removed by an adaptive notch filter, the tails become heavier. The second, collected near a shrimp bed, has extremely heavy tails and a kurtosis (normalized fourth moment) of 82. Excellent results are achieved through use of a Johnson noise model fit.

§1 The Gauss/Gauss Mixture Model

One possible non-Gaussian noise model to consider is the simple mixture [1]. We will assume that both the nominal and contaminant are Gaussian:

$$f(x) = (1-\epsilon) \frac{1}{\sqrt{2\pi}\sigma_1} e^{-\frac{x^2}{2\sigma_1^2}} + \epsilon \frac{1}{\sqrt{2\pi}\sigma_2} e^{-\frac{x^2}{2\sigma_2^2}}$$

where, of course, we are assuming zero mean.

To use such a density one must be able to estimate the parameters of the mixture model. Many methods are possible, for example the Moment Generating Function (MGF) method in which the MGF is estimated at certain discrete points and a close parametric fit is found numerically [2]. We will use the Method of Moments, in which parameters are matched to moment estimates. There are three unknown parameters in the model, so it is necessary to calculate three moments. It is easy to show [3] that the parameters can be found explicitly as:

$$\sigma_1^2 = \frac{1}{2a} [-b + \sqrt{b^2 - 4ac}]$$

$$\sigma_2^2 = \frac{e_4/3 - \sigma_1^2}{1 - \sigma_1^2}$$

$$\epsilon = \frac{1 - \sigma_1^2}{\sigma_2^2 - \sigma_1^2}$$

where

$$a = 1 - e_4/3$$

$$b = e_6/15 - e_4/3$$

89

2 28 017

$$c = (e_4/3)^2 - e_6/15$$

and e_i is an estimate of the i^{th} moment of the noise process, which is assumed to have been normalized to unity variance. It is the explicit nature of the above parameter estimation which is one of the most attractive features of the Gauss/Gauss mixture. Most others (for example the Huber mixture) do not have the property of being easy to estimate. We note in passing that the kurtosis κ achievable with a (σ_1, σ_2) mixture is bounded as

$$\kappa \geq 3 \quad \text{with equality when } \epsilon=0,1 \quad \text{or when } \sigma_1=\sigma_2$$

$$\kappa \leq \frac{(\sigma_1^2 + \sigma_2^2)^2}{4\sigma_1^2\sigma_2^2} \quad \text{with equality when } \epsilon = \frac{\sigma_1^2}{\sigma_1^2 + \sigma_2^2}$$

We see that the Gauss/Gauss mixture may in some cases be a good model for noise with heavier tails than Gaussian.

The Neyman-Pearson optimal nonlinearity for the Gauss/Gauss mixture can be written

$$\psi_{GG}(x) = \log \left[\frac{\frac{1}{\sigma_1} \exp \left(\frac{-(x-s)^2}{2\sigma_1^2} \right) + \frac{1}{\sigma_2} \exp \left(\frac{-(x-s)^2}{2\sigma_2^2} \right)}{\frac{1}{\sigma_1} \exp \left(\frac{-x^2}{2\sigma_1^2} \right) + \frac{1}{\sigma_2} \exp \left(\frac{-x^2}{2\sigma_2^2} \right)} \right]$$

§2 The Johnson Model

Johnson noise [4,5] can be visualized as unit-power Gaussian noise which has been passed through a memoryless and invertible nonlinearity $g^{-1}(\cdot)$. Actually, almost any i.i.d. process can be thought of as being produced in such a way, the Johnson case being special in that the nonlinearity $g^{-1}(\cdot)$ has a simple, explicit form:

$$g^{-1}(z) = \lambda \sinh\left(\frac{z}{\delta}\right)$$

Since the parameter δ has more control over the tail (i.e. large argument) behavior than does λ , it is customary to refer to it as the *tail parameter*. The other parameter λ is a normalizing constant by which, for a given δ , one can set the variance σ^2 of the process.

It can be seen that for constant σ^2 a large value of δ produces essentially Gaussian noise, while a small value causes the density to have heavy tails. In practice we see that $\delta > 5$ produces approximately Gaussian densities, while $\delta < 2$ characterizes very heavy-tailed densities.

As with the mixture model it is important to be able to estimate the parameters, and as with the mixture model we have developed a Method of Moments fit. In the Johnson case we see there are only two parameters to calculate, so we need only two moments, the second and fourth. We can derive [3] a moment estimate of parameters:

$$\delta = \left(\frac{2}{\log(\sqrt{2\kappa-2}-1)} \right)^{\frac{1}{2}}$$

$$\lambda = \left(\frac{2\sigma^2}{\sqrt{2\kappa-2}-2} \right)^{\frac{1}{2}}$$

where σ^2 is the variance and κ the kurtosis. This is possibly a simpler calculation than for the Gauss/Gauss mixture.

The Johnson density has the form

$$f(x) = |g'(x)| \phi(g(x))$$

where $\phi(\cdot)$ is the unit normal and g is the inverse of the sinh nonlinearity:

A-1

$$g(x) = \delta \log \left(\frac{x}{\lambda} + \sqrt{\left(\frac{x}{\lambda}\right)^2 + 1} \right)$$

and

$$g'(x) = \frac{\delta}{\lambda \sqrt{\left(\frac{x}{\lambda}\right)^2 + 1}}$$

The Neyman-Pearson optimal nonlinearity in the presence of an additive signal c can be written most easily as

$$\psi_J(x) = \log \left(\frac{g'(x-c)}{g'(x)} \right) - \frac{1}{2} \left([g(x-c)]^2 - [g(x)]^2 \right)$$

It can be shown that Johnson nonlinearities blank large observations; that is, in the large-amplitude limit, they are zero.

§3 Merchant Shipping Noise

This data set was collected from a single microphone suspended in the Indian Ocean near a merchant shipping lane. The sampling rate used was 1250 data points/second, and 102500 samples were taken, giving a total record length of 82 seconds.

A moment analysis of the raw data gives us the following table:

Moments of Raw Data	
mean	0.023
std dev	544.0
skewness	0.014
kurtosis	2.25

There does not seem to be any reason to assume the noise to be non-stationary.

A spectrum analysis of the noise was performed, with results shown in Figure 3.1. Instead of a broadband or low-pass characteristic, the spectrum has a strong peak around 90-100 Hz, smeared over a band of about 50 Hz. Returning to the physical system we see that this is not remarkable. This relatively high frequency tone is more likely due to vibrations in the structure of the ship, than to the rotation of the engine itself. This is also suggested by small peaks at harmonic frequencies of the heavy tone, pointing to the nonlinear nature of the device producing the tone, and suggestive of mechanical vibration.

A substantial part of the noise power is in this tone, as can be seen from the empirical spectrum, the small value of kurtosis, and light-tailed probability plot. The removal of this tone would very likely make a radical difference in the statistics of the process, since we expect to be able to remove the effect of the passing ship and deal only with ambient noise. An ideal device to accomplish this separation is the Adaptive Notch Filter.

An adaptive notch filter [6] functions by placing the deepest part of its notch over the highest amplitude section of the noise spectrum. In the common spectral-analysis test model of sinusoids in white noise, the notch will naturally place itself to reject the sinusoid. In its full generality the ANF can include many cascaded stages to reject many sinusoids. A gradient algorithm controls the adaptation and seeks to minimize output power. Considerations about convergence, and modifications to the filter which can enhance it will not be treated here; initial convergence can often be quite slow. In our case we will ignore this problem by initializing the filter to a nearly-optimal value.

The form of the filter is

$$H(z) = \frac{z^2 + bz + 1}{z^2 + \alpha bz + \alpha^2}$$

It is easy to show that this is a notch filter with

$$\text{center frequency} = \cos^{-1}\left(-\frac{b}{2}\right)$$

and

$$\text{band-width} \sim 2(1-\alpha)$$

The adaptation is accomplished through updating b :

$$b_{n+1} = b_n - \mu y_n (x_{n-1} - \alpha y_{n-1})$$

where μ is a constant which trades stability for speed of convergence. A typical value for μ is $(1-\alpha)/10$.

Adaptive notch filters were applied to the raw data in an attempt to remove the noise from the ship. The effects of several notch widths on the probability distribution of the data are shown in Figure 3.2; the noise in each case has been normalized to unit variance and zero mean. As the notch became wider the distribution developed heavier tails. As the parameter α dropped below .80 very little further effect was seen on the distribution; this value of α corresponds to a notch width of 80 Hz and is of the same order but slightly larger than the width of the smeared peak in Figure 3.1. That $\alpha < .80$ corresponds to an unnecessarily sloppy notch is confirmed in Figure 3.3, a plot of output power versus α . Qualitatively we observe that for $\alpha > .95$ the filter removes too little of the ship's noise; the improvements are unimpressive for $\alpha < .80$, and in a practical situation such a filter could remove too much signal power to be worthwhile.

This work suggests the following model for merchant shipping noise X_n :

$$X_n = Y_n + Z_n$$

where Y_n is a high power, narrowband process centered around 94 Hz., and probably due to mechanical vibration in the nearby ship; and Z_n is a lower power, more broad-band process with somewhat heavier-than-Gaussian tails, possibly unrelated to the ship. An empirical probability plot of the output of the ANF with $\alpha = .90$ is shown in Figure 3.4.

The application of these studies and models is to be able to detect a known signal $\{c_i\}$ in noise. Several detectors have been implemented.

[D1] The Linear Detector.

[D2] The Gauss/Gauss Mixture Detector.

The parameters:

$$\epsilon = 0.0371 \quad \sigma_1 = 483 \quad \sigma_2 = 1050$$

are the same as in [2].

[D3] The amplifier-limiter.

This detector limits input amplitudes to $\pm 2\sigma$, and was included after [2].

[D4] The Notch-Linear Detector.

This detector is simply D1 where observations have been pre-processed by a notch filter with $\alpha = .90$. Owing to the interference of signal with adaptation, a non-adaptive notch filter with center frequency 94 Hz was used. In practice, this scheme would have to be used with the signal random, or frequency-hopped, or weak, or some scheme to avoid having the ANF cancel the signal. There is not enough data present to test such a procedure adequately in the present situation.

The simulations were performed as follows. The noise power was estimated and used to obtain a sample-by-sample SNR of 0dB. A constant signal was used, after [2], and also to avoid a situation where the signal spectrum was too optimistically or too pessimistically placed with respect to the noise spectrum (for example, a non-vanishing alternating signal could be detected with almost unity power). The record length was chosen as 10, allowing approximately 10000 repetitions per detector. Note that observations were made down to $\alpha = 10^{-4}$, but only those where $\alpha > 10^{-3}$ were considered reliable. (The notation is standard but

regrettable: now that we are not dealing with notch filters, α is used to mean probability of false-alarm.)

The results were as shown in Figure 3.5. The linear detector (D1) outperformed both the mixture detector (D2) and the amplifier-limiter. This is not surprising considering that the latter two are optimal for noise with heavier-than-Gaussian tails, and this data set has lighter-than-Gaussian tails. Pre-processing the data by a notch-filter offered a dramatic improvement over the first three detectors. A further simulation, shown in Figure 3.6, demonstrates the effect of widening the notch on detector performance.

As suggested earlier by Figure 3.4, the output from the notch filter has slightly heavier-than-Gaussian tails, and a parametric fit can be achieved. A further simulation was performed to see if there were any significant improvement from the increased sophistication of the model. This included detectors:

[D5] The Notch-Mixture Detector.

The output of the notch filter was passed through a mixture nonlinearity with parameters

$$\epsilon=.33 \quad \sigma_1=337 \quad \sigma_2=401$$

[D6] The Notch-Johnson Detector.

The output of the notch filter was passed through a Johnson nonlinearity with parameters

$$\delta=6.79 \quad \lambda=2410$$

The results indicate that very little improvement is achieved [3].

§4 Shrimp Noise

This data set was collected in the Pacific Ocean off Hawaii, near a concentration of shrimp. The sampling rate used was 40000 data points/second, and 96000 samples were taken, giving a total record length of 2.4 seconds.

A moment analysis of the raw data gives us

Moments of Raw Data	
mean	1.79
std dev	48.3
skewness	0.089
kurtosis	82.5

This is characteristic of a highly non-Gaussian environment; the density has extremely heavy tails. A probability plot drawn in Figure 4.1 confirms this: approximately one out of ten thousand observations will have amplitude greater than 16σ .

In this figure the Gauss/Gauss mixture and Johnson fits are also presented. The relevant parameters are for the mixture

$$\epsilon=.00165 \quad \sigma_1=43.4 \quad \sigma_2=563$$

and for the Johnson system

$$\delta=.901 \quad \lambda=20.8$$

It is apparent that the mixture fit is not acceptable. For such heavy-tailed noise, the probability plot is forced to develop a 'knee' (around 3.5σ) which is not present at all in the empirical distribution. The Johnson fit on the other hand is quite good, at least up to a tail weight

of 10^{-4} . Beyond that, shrimp noise is heavier-tailed than the Johnson fit, although the fit does not seem to be degrading quite as rapidly as for the Gauss/Gauss mixture. It is clear that the Johnson density is a good sub-optimal parametric choice.

The physical system producing this noise sequence is a nearby school of shrimp. To communicate with each other (and presumably to attract a mate) these creatures snap their claws rapidly, producing loud 'clicks'. A noise sequence from sample 10001–20000 is shown in Figure 4.2a. In this plot there are easily-recognizable high-amplitude events, of about two to five milliseconds duration, occurring against a more well-behaved background. Unfortunately, although in this record the clicks are loud and of reasonable length, the next record (samples 20001–30000, Figure 4.2b) demonstrates that this is not always the case. There are several overt clicks, and also many high-amplitude observations which seem to be isolated. The reason for these isolated observations is not clear; we can speculate that the longer-duration clicks are produced differently by the shrimp themselves. We also note a tendency (which is unfortunately not a rule) for two events to occur within a space of 10–30 ms or so, perhaps a result of both claws being exercised.

The difficulty in characterizing high-amplitude observations into well-behaved bursts makes makes recognition of mode-changes complicated. It was decided, due to the heavy-tailed nature of the noise, to attempt to separate clicks from background noise using the non-parametric burst detector [7]. Such a device functions by deciding on a sample-by-sample basis (i.e. by a simple threshold) from which mode a data point comes, and subsequently smoothing this estimate using a median filter. Figure 4.3 gives close-up views of fairly typical well-defined clicks. It was decided to use a median filter of length 61 since that is the approximate length of the shorter clicks. The short median filter necessary to detect such quick bursts can lead to too many spurious mode-changes, so a fairly high threshold of twice the standard deviation was used.

In order to compensate for the varying burst-strength (probably due to the proximity of the source shrimp), each burst in the "high" mode has been normalized to have the same variance. This empirical approach to mode separation has had some success: the tails on both the high- and low-variance modes have been reduced. This can be seen from the separated moment and Johnson parameters

Moment and Johnson Parameters				
	Original	Analysis After Separation		
		Low	High	Raw High
std dev	48.3	35.1	-	110.0
kurtosis	82.5	4.47	4.90	28.2
δ	0.90	2.01	1.85	1.03
λ	20.8	62.3	-	67.1

The "high" mode data does not of course contain any relevant amplitude-related parameters. The "raw high" column refers to non-normalized bursts and shows us that a simple (i.e. multiplicative) burst detector is not optimal in this situation.

The non-stationary nature of shrimp noise makes observations about time dependence difficult and perhaps not very meaningful; however, we show the spectrum in Figure 4.4. There is a very sharp rise at 2.5 kHz and a steady drop-off, with some evidence of a harmonic tone around 5 kHz. The plot's lack of smoothness, despite the application of a Parzen window, attest to the unmanageability of this data set. It also appears that sampling was done at something below the Nyquist frequency, although it is not clear that a reasonable one exists for this environment. For the earlier Figure 4.3, it was observed that a burst seemed somewhat tonal (around 2.5 kHz): to examine this hypothesis the high- and low-variance modes were treated separately. In each case, data records of length 64 (this low length was chosen due to the difficulty of finding long bursts) were transformed, squared, and averaged; the results are shown in Figure 4.5. The bursts appear considerably more tonal and band-limited in nature than the background mode, and indeed the small 2.5 kHz peak in the low-variance mode may be due to imperfections in the mode-separation algorithm.

The simple detection described in the Merchant Shipping Noise section was posed in this noise environment to compare several detection schemes. These were:

[D1] The Linear Detector.

[D2] The Gauss/Gauss Mixture Detector.

[D3] The Laplace Noise Detector.

[D4] The Johnson Noise Detector.

[D5] The Mode-Switched Johnson Detector.

Ideally to use this detector the two modes should, after removal of a multiplicative constant, have identical densities. Since this is not the case here, the more pessimistic 'raw high mode' values of

$$\delta=1.03 \quad \lambda=67.1$$

were used here. The non-parametric mode-detector described earlier controlled pre-multiplication: observations judged to have come from the high-variance mode were multiplied by one third, the approximate ratio of the standard deviations of the two modes.

In each case a sample-by-sample signal to noise ratio of 0 dB was used, a constant signal, and a detection record length of 5. The results of this experiment were rather as expected. As shown in Figure 4.6, the linear detector (D1) performed extremely poorly. The Johnson detector performed well, better than the Gauss/Gauss mixture detector (D2) or the Laplace detector (D3) (although this was quite good) as was expected from its good distributional fit. The mode-switched Johnson detector (D5) was the best simulated although due to burst-estimation problems the performance deteriorated for small probabilities of false-alarm. It is a somewhat unsatisfying system to use, however, due to the necessity to specify parameters of burst length and threshold, and the difficulty of burst-detection in the presence of a non-vanishing signal. It would seem that the Johnson detector is perhaps the wisest choice in this environment.

§5 Summary

The analysis of the previous data sets has suggested, among others, the following insights.

The Johnson detector seems dependably good, and is particularly attractive since its two parameters can be estimated explicitly through the variance and kurtosis statistics (this of course assumes zero-mean, symmetric densities).

The application of a notch filter to the data stream seems often to be an easy way to improve performance, since two of the three records studied were dominated by a single tone. However, we note that care must be taken in the case of an *adaptive* notch filter, due to the unavoidable tendency of this device to cancel the received signal itself, given a narrowband signal with sufficient power. Random signals, frequency-hopped or swept signals, or a noise-alone channel would give practical inputs for such a system. The simulations presented were performed using a fixed notch filter.

The use of burst detectors seems to improve performance dramatically. However, these devices are difficult to implement in the presence of a non-vanishing signal; again, in the simulations the modes were estimated offline. Also, it was difficult to make such a system error-free, causing the performance to deteriorate to no better (or worse) than memoryless systems for low probabilities of error.

There are clearly many avenues for further research. The good performance of the Johnson detector suggests that it is not vital to have the precisely optimal density estimate in order to have a good detector. It seems possible that the complex Johnson nonlinearity could be simplified through use of some piecewise fit with little degradation in performance. Also,

some study of the performance of the adaptive notch filter in the presence of a non-vanishing signal should be undertaken.

It would be valuable to improve the performance of the switched-burst detector by recognizing the imperfect nature of the switch-estimator; the resulting detector would be forced to develop a more robust low-variance-mode nonlinearity. Finally, it seems generally true that bursts are seldom white, but are more frequently narrowband. Switch-estimators, on the other hand, tend to assume bursts of white noise. One approach to estimation of highly-correlated bursts is to decimate; it would seem that a more rigorous statistical calculation might lead to a different approach with superior performance.

§6 Acknowledgment

This work was supported in part by the Office of Naval Research under Grant N00014-81-K-0146 and in part by the National Science Foundation under Grant ECS83-17777.

§7 References

- [1] J.H. Miller and J.B. Thomas, "The Detection of Signals in Impulsive Noise Modelled as a Mixture Process" *IEEE Transactions on Communications*, Vol COM-24, pp. 559-563, May 1976.
- [2] M. Bouvet and S.C. Schwartz, "Underwater Noises: Statistical Modelling, Detection, and Normalization", *submitted to Journal of the Acoustical Society of America*, 1986.
- [3] P. Willett, "Density Representations with Applications to Signal Detection", *PhD Thesis, Princeton University*, 1986.
- [4] E. Modugno, "The Detection of Signals in Impulsive Noise", *PhD Thesis, Princeton University*, 1982.
- [5] N. Johnson, "Systems of Frequency Curves Generated by Methods of Translation", *Biometrika*, Vol 36, pp. 149-176, 1949.
- [6] S. Czarnecki, "Nearly-Optimal Detection of Signals in Non-Gaussian Noise", *PhD Thesis Princeton University*, 1983.
- [7] L. Pearlstein and B. Liu, "Retrieval of Sinusoidal Signals by Adaptive Notch Filtering", *Proceedings of the Twenty-Third Annual Allerton Conference on Communications, Control, and Computing*, pp. 574-583, 1985.

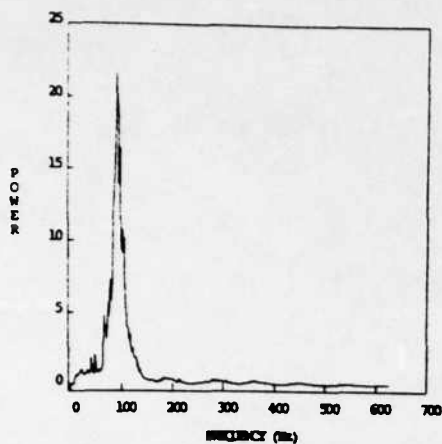


Fig. 3.1 (Merchant) Spectrum

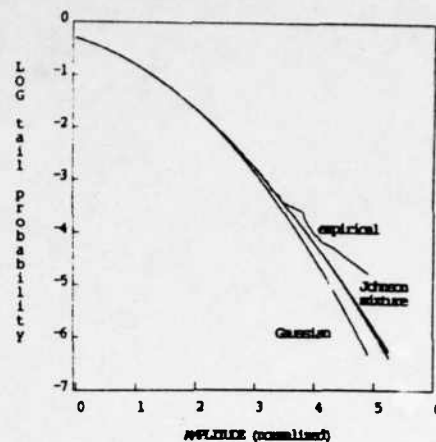


Fig 3.4 (Merchant) PDF with $\alpha=.90$

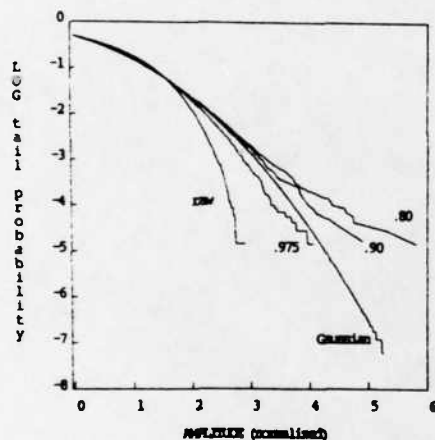


Fig. 3.2 (Merchant) PDF vs. α

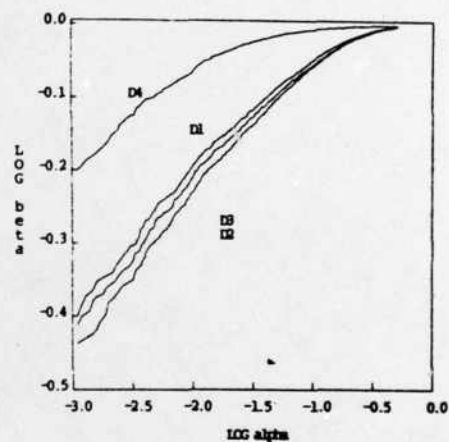


Fig 3.5 (Merchant) ROC

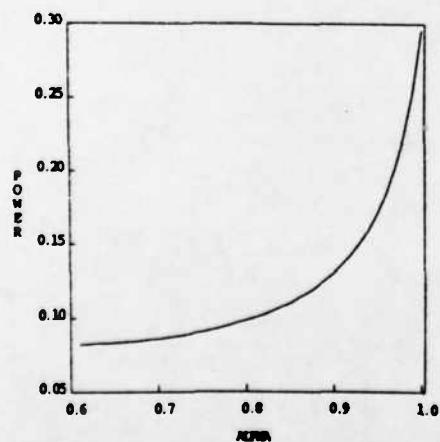


Fig. 3.3 (Merchant) Power vs. α

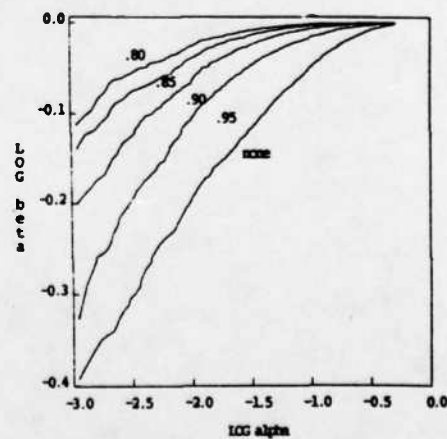


Fig 3.6 (Merchant) ROC vs. α of ANF

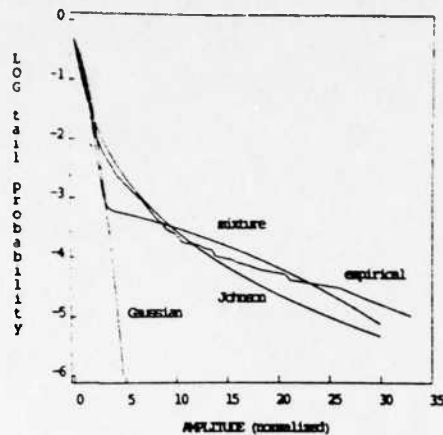


Fig 4.1 (Shrimp) PDF

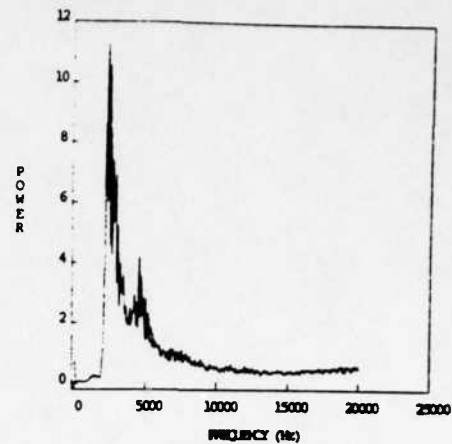


Fig 4.4 (Shrimp) Spectrum

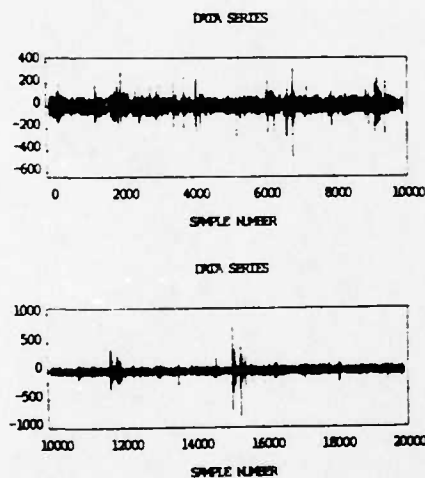


Fig 4.2 (Shrimp) Data Samples

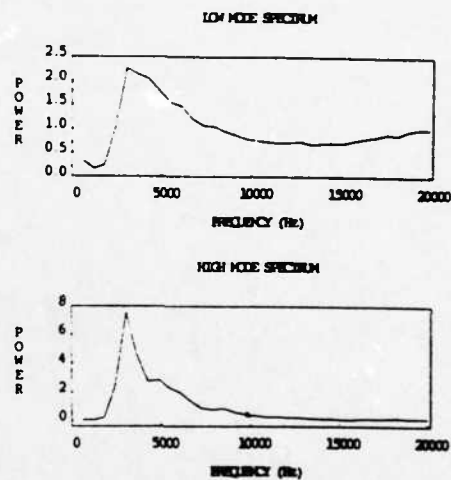


Fig 4.5 (Shrimp) Spectrum after Mode-Separation

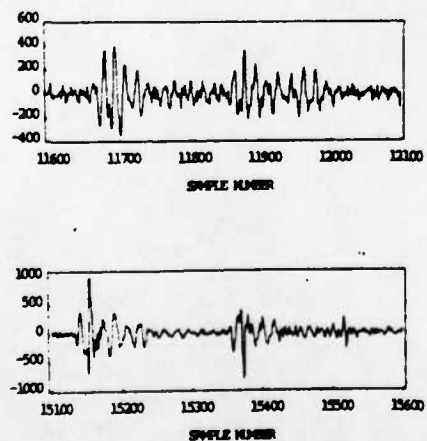


Fig 4.3 (Shrimp) Well-Defined "Clicks"

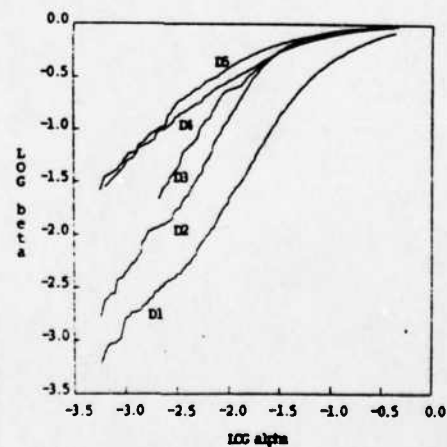


Fig 4.6 (Shrimp) ROC

DTIC

FILMED

4-89